STATISTICAL EMISSION PROPERTIES OF A NONRESONANT FEEDBACK LASER

R. V. AMBARTSUMYAN, P. G. KRYUKOV, V. S. LETOKHOV, and Yu. A. MATVEETS

P. N. Lebedev Physics Institute, Academy of Sciences, USSR

Submitted July 14, 1967

Zh. Eksp. Teor. Fiz. **53**, 1955–1966 (December, 1967)

Statistical properties of emission from a nonresonant feedback laser are investigated theretically and experimentally. It is shown that the intensity of laser emission in a narrow solid angle corresponding to a single mode is subject to strong fluctuations whose distribution function coincides with the Bose-Einstein distribution for black-body radiation. The distribution function for the total number of photons in all the laser modes (within the complete solid angle) is determined. This dispersion of the fluctuation of the total number of photons is much smaller than in the case of black-body radiation in the same number of modes.

INTRODUCTION

A nonresonant feedback laser was suggested and studied previously[1,2]. Nonresonant feedback was produced in[1,2] by a scatterer substituting for one of the Fabry-Perot resonator mirrors. The scattering caused a strong interaction between a large number of modes with different wave vectors with the result that the resonant properties of the Fabry-Perot resonator vanished. In other words, the standing waves that are usually established within the laser were replaced by a spatially random field that interacted with the active medium as a whole.

The emission properties of a nonresonant feedback laser differ from those of ordinary lasers. First of all this applies to the emission spectrum. The generation spectrum is continuous and free of the typical discrete components at the resonant frequencies of the resonator. After the threshold is reached the generation spectrum continuously "shrinks" toward the center of the amplification line of the active medium and, in the ideal case, the limiting spectral width is determined by fluctuations[3]. It was noted in[3] that the emission statistics of a nonresonant feedback laser should differ significantly from that of ordinary lasers. This hypothesis is confirmed by the results of theoretical and experimental investigation of the statistical properties of the emission of such a laser presented in this paper. The preliminary results of this research were published in[4].

The theoretical investigation was based on the method of governing equations for the probabilities of states in a system consisting of M two-level atoms and L modes. The governing equations for the case of multimode emission were obtained in[5]. They represent a generalization of the governing equations obtained by Fleck[6,7] for the case of a single mode. In our case of a nonresonant feedback laser the governing equations of[5] are supplemented by terms that phenomenologically describe mode interaction through scattering photon exchange. The solution of governing equations in the stationary case yields distribution functions of the total number of photons N in all generation modes and the number of photons n in a single mode of a set of L modes. It is shown that the statistics of photon fluctuation in a single mode of laser emission is the same as in black-body radiation; however the fluctuations of the total number of photons in all modes have a much smaller dispersion than does the black-body radiation in the same number of modes.

A pulse ruby laser with nonresonant feedback having $L \approx 10^6$ modes was used in the experiments. The experimentally determined distribution function of the number of photons in a single mode is in good agreement with theory.

The decrease of dispersion of photon fluctuation with increased number of modes was investigated. The resulting dependence is in a qualitative agreement with theory. The correlation radius (area of coherence) and correlation time (coherence time) of the emission fluctuation were determined and compared with theory.

THEORETICAL ANALYSIS

1. The Model

We consider the following model of a nonresonant feedback laser. The ensemble M of two-level atoms with negative temperature is contained in a "stochastic resonator." The term "stochastic resonator" means any cavity having a large number of interacting modes (waves in different directions) with the same attenuation. This can be realized in practice by a system consisting of a mirror with diameter D and a scatterer[1)] at a distance l from the mirror (provided that $D^2/\lambda l \gg 1$)[1,2] or an aggregate of scattering particles[10]. The number of modes L coupled by scattering is determined by

$$L \approx \Omega_{\text{gen}}/\Omega_{\text{diff}}, \tag{1}$$

where Ω_{gen} is the solid angle of the generated emission and $\Omega_{\text{diff}} \approx (\lambda/D)^2$ is the solid diffraction angle. The spectral density P_ω of the modes and the mean distance between the modes $\delta_\omega = P_\omega^{-1}$ as given by Raleigh-Jeans equation are

$$P_\omega = L\frac{2l}{c}, \quad \delta\omega = \frac{c}{2l}\frac{1}{L}. \tag{2}$$

During scattering the emission is transferred from one mode into the remaining $L - 1$ modes or into open space. The escape of emission into the modes of the "stochastic resonator" does not entail energy losses

[1)]The scatterer may also comprise various inhomogeneities in the active medium itself.

for the system as a whole but results in mode interaction. The emission loss rate Γ in a mode due to transfer to the other $L-1$ modes is determined by

$$\Gamma=\frac{c}{2l}\ln\left(\frac{1}{\alpha r}\frac{\Omega_{\text{gen}}}{\Omega_{\text{diff}}}\right)=\frac{c}{2l}\ln\left(\frac{L}{\alpha r}\right), \tag{3}$$

where α is the scatterer albedo and r is the reflection coefficient of the mirror. The escape of emission into open space determines the radiation losses of the system. The emission loss rate γ due to this process is

$$\gamma=\frac{c}{2l}\ln\left(\frac{1}{\alpha r}\frac{\Omega_{\text{scatt}}}{\Omega_{\text{gen}}}\right), \tag{4}$$

where Ω_{scatt} is the solid angle of the back scattering assuming that $\Omega_{\text{scatt}} \gg \Omega_{\text{gen}}$.

Using the introduced damping constants we write the condition for nonresonant feedback as follows:

$$\Gamma, \gamma \gg \delta\omega. \tag{5}$$

The necessary condition for (5) is that $L \gg 1$.

2. Governing Equation for $P^{n,N}$

The state of the system "emission in L modes + ensemble M of two-level atoms" is characterized by the number m of atoms at the lower level, the number n_l of photons in l-th mode, and the total number of photons in all modes $N = \Sigma n_l$ (summation over $l = 1 \ldots L$). For simplicity all modes are considered identical. This means that the constants of emission-atom interaction k and loss attenuation γ are the same for all modes. Furthermore we consider the case for which the average frequency of emission is the same in all modes. This assumption is a priori valid when generation is close to the stationary state so that the spectral width of the emission $\Delta\omega \ll \gamma, \Gamma$. Then the total probability $P_m^{n_l,N}$ of states with n_l photons in the l-th mode, on condition that N photons are in all L modes and m atoms are at the lower level, is expressed by the governing equation derived in[5]:

$$\begin{aligned}\dot{P}_m^{n_l,N} = & -k(N+L)(M-m)P_m^{n_l,N} + k(m+1)(N-n_l+1)P_{m+1}^{n_l,N+1} \\ & + k(m+1)(n_l+1)P_{m+1}^{n_l+1,N+1} - kNmP_m^{n_l,N} + k(M-m+1) \\ & \times (N-n_l+L-2)P_{m-1}^{n_l,N-1} + k(M-m+1)n_lP_{m-1}^{n_l-1,N-1} \\ & + S(M-m+1)P_{m-1}^{n_l,N} - S(M-m)P_m^{n_l,N} - \mathscr{P}mP_m^{n_l,N} + \mathscr{P}(m+1)P_{m+1}^{n_l,N} \\ & + \gamma(N+1-n_l)P_m^{n_l,N+1} + \gamma(n_l+1)P_m^{n_l+1,N+1} - \gamma NP_N^{n_l,N},\end{aligned} \tag{6}$$

where $k = \sigma c/V$ (σ is the cross section of radiative transition of atoms, V is the resonator volume, and c is the velocity of light), S is the de-excitation probability of an atom, $\mathscr{P}$ is the excitation probability of an atom due to pumping, and γ is determined by (4).

The governing equation (6) must include incoherent interaction of modes due to photon exchange. The mode interaction is described phenomenologically by the probability of photon arrival Γ' at a mode from the remaining $L-1$ modes and the probability of photon departure Γ from a mode to the remaining $L-1$ modes. Then the total change in probability due to photon exchange between the l-th mode and the remaining $L-1$ modes can be written in the form

$$\dot{P}_m^{n_l,N} = \Gamma[(n_l+1)P_m^{n_l+1,N} - n_lP_m^{n_l,N}] + \Gamma'[n_lP_m^{n_l-1,N} - (n_l+1)P_m^{n_l,N}]. \tag{7}$$

In (7) we take into account the fact that the photon exchange among the modes does not affect the total number N of photons in all the modes.

The rates of departure Γ and arrival Γ' of photons in a mode obey the condition that the intermode photon exchange does not change the average number of photons in a mode $\langle n_l \rangle$. This condition has the form

$$\begin{aligned}\frac{d\langle n_l\rangle}{dt} = \frac{d}{dt}\sum_{n_l, m, N} n_lP_m^{n_l,N} = -\Gamma\sum_{n_l, m, N} n_lP_m^{n_l,N} + \\ + \Gamma'\sum_{n_l, m, N}(n_l+1)P_m^{n_l,N} = -\Gamma\langle n_l\rangle + \Gamma'\langle n_l+1\rangle = 0.\end{aligned} \tag{8}$$

Consequently

$$\Gamma' = \frac{\langle n_l\rangle}{1+\langle n_l\rangle}\Gamma. \tag{9}$$

The governing equation (6) with the interaction terms (7) completely defines the statistics of emission of the nonresonant feedback laser model under consideration.

3. Distribution of the Total Number of Photons

The governing equation for the probability P^N of detecting N photons in all the modes can be obtained by a summation over n_l and m in the governing equation (6) with the mode interaction terms (7):

$$\begin{aligned}\dot{P}^N = & -kM(N+L)\eta_a(N)P^N + kM(N+1)\eta_b(N+1)P^{N+1} \\ & - kMN\eta_b(N)P^N + kM(N+L-1)\eta_a(N-1)P^{N-1} \\ & + \gamma(N+1)P^{N+1} - \gamma NP^N,\end{aligned} \tag{10}$$

where $\eta_a(N)$ and $\eta_b(N)$ are the relative probabilities of populating the upper and lower levels of atoms given the presence of N photons in all modes.

In the stationary case ($\dot{P}^N = 0$) Eq. (10) has a general solution[5]:

$$P^{N+1} = \frac{N+L}{N+1}\frac{kM\eta_a(N)}{\gamma + kM\eta_b(N+1)}P^N, \tag{11}$$

and the relative probabilities $\eta_a(N)$ and $\eta_b(N)$ are determined by the relationships[5]

$$\eta_a(N) = \frac{\mathscr{P}+kN}{\mathscr{P}+S+k(2N+L)}, \quad \eta_b(N) = \frac{S+k(N+L)}{\mathscr{P}+S+k(2N+L)}. \tag{12}$$

Of the greatest practical interest is the range of values $N \gg 1$ in which the recurrent relation (11) can be replaced by the differential equation

$$\frac{dP^N}{dN} = f(N)P^N, \quad f(N) = \frac{N+L}{N+1}\frac{kM\eta_a(N)}{\gamma + kM\eta_b(N+1)} - 1. \tag{13}$$

The distribution P^N reaches a maximum at the point $N = \overline{N} \approx \langle N \rangle$ determined from the condition $f(\overline{N}) = 0$. When $\langle N \rangle L^{-1} \gg kM/\gamma\zeta$ the expression for $\langle N \rangle$ has the form

$$\langle N\rangle = \frac{\mathscr{P}+S+kL}{2k}(\zeta - 1), \tag{14}$$

where ζ is the coefficient of pump excess over threshold that is determined by the relation

$$\zeta = \frac{\mathscr{P}-S-kL}{\mathscr{P}+S+kL}\frac{kM}{\gamma}. \tag{15}$$

Expanding $f(N)$ about the point $N = \langle N \rangle$ and taking only the first term of the expansion ($L, \langle N \rangle \gg 1$), we find the following expression for P^N:

$$P^N = \frac{1}{\sigma\sqrt{2\pi}}\exp\left[-\frac{(N-\langle N\rangle)^2}{2\sigma^2}\right], \tag{16}$$

where σ^2 is the dispersion of fluctuations of the total number of photons N that is determined by the expression

$$\sigma^2 = \left[\frac{L-1}{\langle N\rangle(\langle N\rangle + L)} + \frac{2\gamma}{M(\mathcal{P} + k\langle N\rangle)} \right]^{-1} \quad (17)$$

The basic difference of the distribution P^N for the nonresonant feedback laser emission from the corresponding distribution P^N for a black-body radiation[5] consists in a significant reduction of the dispersion of the total photon number fluctuation. This effect is determined by the second term in (17) and can be physically interpreted as due to the stabilizing effect of saturation in the stationary generation regime.

4. Photon Distribution in a Single Mode

A summation over m and N in the initial governing equation (6) and (7) yields the following equation for the probabilities P^{n_l} of detecting n_l photons in the l-th mode of a set of modes:

$$\begin{aligned}\dot{P}^{n_l} = &-kM(n_l+1)\eta_a'(n_l)P^{n_l} + kM(n_l+1)\eta_b'(n_l+1)P^{n_l+1} \\ &- kMn_l\eta_b'(n_l)P^{n_l} + kMn_l\eta_a'(n_l-1)P^{n_l-1} \\ &+ (\gamma+\Gamma)\left[(n_l+1)P^{n_l+1} - n_lP^{n_l}\right] + \Gamma'\left[n_lP^{n_l-1} - (n_l+1)P^{n_l}\right],\end{aligned} \quad (18)$$

where $\eta_a'(n_l)$ and $\eta_b'(n_l)$ are the relative probabilities of populating the upper and lower levels of atoms given the presence of n_l photons in the l-the mode. In deriving (18) we used the fact that the total number of photons N in all the modes is subject to relatively small fluctuations (Sec. 3) and the resulting sums can therefore be simplified as follows:

$$\sum_{m,N} NP_m^{n_l\ N} = \langle N\rangle P^{n_l}. \quad (19)$$

A general solution of the governing Eq. (18) in the stationary case has the form

$$P^{n_l} = \prod_{n'=0}^{n_l-1} \left[\frac{\Gamma' + kM\eta_a'(n')}{\gamma + \Gamma + kM\eta_b'(n'+1)} \right] P^0. \quad (20)$$

As in the case of nonequilibrium multimode radiation[5] we can show that in our case the relative probabilities η_a' and η_b' do not depend on n_l but are determined by the total number of photons N. The distribution (20) is then reduced to

$$P^{n_l} = \left[\frac{\Gamma' + kM\eta_a(\langle N\rangle)}{\gamma + \Gamma + kM\eta_b(\langle N\rangle)} \right]^{n_l} P^0, \quad (21)$$

where η_a and η_b are determined by (12). It follows from $f(\langle N\rangle) = 0$ that

$$\frac{kM\eta_a(\langle N\rangle)}{\gamma + kM\eta_b(\langle N\rangle)} = \frac{\langle N+1\rangle}{\langle N+L\rangle} \approx \frac{\langle n_l\rangle}{1 + \langle n_l\rangle}. \quad (22)$$

Substituting this inequality into (21) and considering that according to (9) the ratio Γ'/Γ is determined by an identical expression, we finally obtain the following expression after normalization:

$$P^{n_l} = \langle n_l\rangle^{n_l} / (1 + \langle n_l\rangle)^{1+n_l}. \quad (23)$$

Thus the distribution of the number of photons in a single mode of a nonresonant feedback laser coincides with the black-body radiation distribution but significantly differs from the photon distribution in a single mode laser. In contrast to the ordinary lasers, in our laser the saturation effect fails to stabilize the number of photons in a single mode. Due to the fact that all the modes generate as a whole, only the total number N of photons in all modes is stabilized (Sec. 3). At the same time a random redistribution of photons among the modes is allowed as long as the total number of photons N remains relatively constant.

The intensity fluctuations in the individual modes are apparently typical for multimode lasers, although they are not as distinct as in the nonresonant feedback laser. For example, Armstrong and Smith[9] observed a considerable correlation of the fluctuations in two modes of a GaAs injection laser that had a relatively stable total number of photons in the two modes. Similar phenomena seem to occur in a multimode argon laser at the transition λ = 4880 Å capable of considerable gain[10]. In those cases however we may have a different mechanism creating these fluctuations. Instead of a direct transition of photons from one mode to another due to scattering, we may be observing gain fluctuations in different modes. On the other hand it is possible that such interactions occur also in nonresonant feedback lasers although they are masked by the strong scattering interaction of the modes.

THE EXPERIMENT

1. The Experimental Setup

Figure 1 shows a diagram of the experimental setup used to study the statistical properties of nonresonant feedback laser emission.

The nonresonant feedback laser consisted of a ruby crystal with a length l = 110 mm and diameter D = 9.5 mm immersed in a liquid-nitrogen dewar and pumped by a helical flash lamp. One end face of the crystal was coated with a mirror having a reflection coefficient $r \approx 50\%$ and the other end was rounded off and ground dull to produce the scattering feedback. The lateral surface of the crystal was also ground dull.

Cooling of the crystal was necessary for the following reasons. The detection of emission fluctuations within a narrow solid angle (in a single mode) requires a sensitive instrumentation with a high time resolution. We had at our disposal a photomultiplier with a time resolution of $\tau \approx (2\text{–}3) \times 10^{-9}$ sec. This instrument allowed for a reliable detection of emission fluctuation with a spectral width of $\Delta\nu \ll \tau/2\pi c$ = 0.015 cm^{-1}. In the pulse generation mode the emission spectrum of a ruby laser at 300°K contracts to 10^{-2} cm^{-1} during a period of 10^{-3} – 10^{-4} sec[3]. A narrower generation line can be obtained by a reduction of the initial width that is determined by the luminescence line width. When the ruby is cooled down to 77°K the luminescence line width decreases by more than an order of magnitude and becomes equal to 0.5 cm^{-1}[11]. In this case we could expect to obtain a generation line with $\Delta\nu \approx 10^{-3}$ cm^{-1}.

The threshold gain per pass K can be obtained from the self-excitation condition for a nonresonant feedback laser[1,2]:

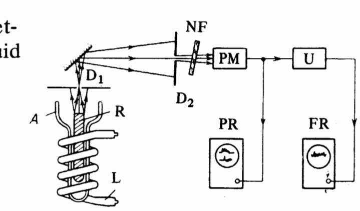

FIG. 1. The experimental setup. R–ruby; A–dewar with liquid nitrogen; L–flash lamp; D_1 and D_2–diaphragms; NF–neutral filter; PM–photomultiplier; U–amplifier; PR–generation pulse recorder (S1-17); FR–fast fluctuation recorder (I2-7).

$$K = \left[\frac{1+\rho}{\alpha r}\frac{\Omega_{scatt}}{\Omega_{gen}}\right]^{1/2} \qquad (24)$$

(ρ is the degree of depolarization of the scattered emission). In our case $\Omega_{scatt} \approx 2\pi$, $\Omega_{gen} \approx (D/l)^2 \approx 10^{-2}$ sr, $\rho \approx 1$, $r \approx 0.5$, $\alpha \approx 0.2$–0.5, and consequently the threshold gain per pass $K \approx 10^2$. The threshold gain per unit length, $\kappa_0 = l^{-1} \ln K = 0.45\ cm^{-1}$, a value readily achievable in a ruby at the liquid nitrogen temperature.

In our experiment the threshold was reached when the voltage of the IFK-15000 pulse lamp was of the order of 5 kV. The crystal was cooled with liquid nitrogen poured into the dewar before every flash. Directly before the flash the nitrogen had to be poured out because it boils vigorously and becomes explosive during a flash discharge. The dewars were periodically replaced because of the intense brief heating produced by a flash that dulled the dewar surface after some time.

Two diaphragms were used to record emission within a narrow solid angle: D_1 with a diameter $d_1 = 0.5$ mm and D_2 with a variable diameter $d_2 = 0.2 - 5$ mm spaced at a distance $h = 60$ cm from each other.

The generation pulse was picked up by an FÉU-15B photomultiplier. Neutral filters used to maintain the light signal at a constant level when the diameter of the second diaphragm was varied were placed in front of the photomultiplier. To register fast intensity fluctuations, the photomultiplier signal was passed through a UZ-5A wideband amplifier with a 150 MHz bandwidth and then to an I2-7 fast oscilloscope. To record the entire generation pulse, the photomultiplier signal was also impressed on one of the beams of the Si-17 two-beam oscilloscope with a 25 MHz bandwidth. The second beam of this oscilloscope was used to mark the starting time of the short sweep of the I2-7 oscilloscope displaying the fast intensity fluctuations. This arrangement allowed us also to measure the average intensity of the generation signal during the short sweep interval.

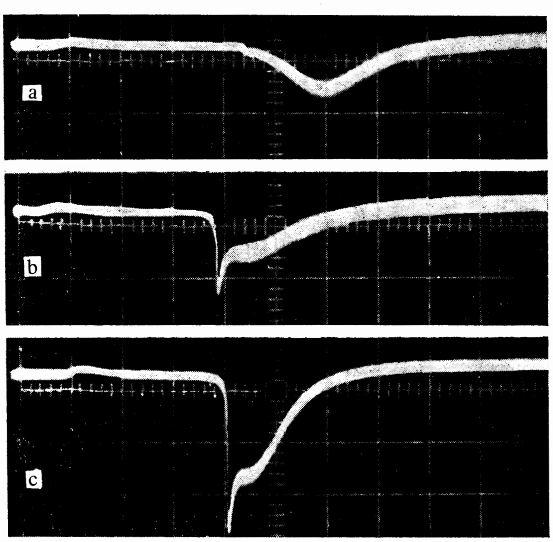

FIG. 2. Oscilloscopic traces of generation pulses at various pump levels: (a) flash lamp voltage U = 5 kV (near threshold); (b) U = 6.5 kV; (c) U = 7 kV. Sweep rate—100 μsec/cm.

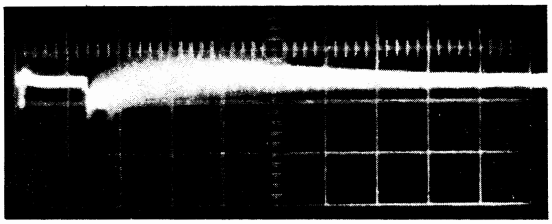

FIG. 3. Oscilloscopic trace of emission pulse in a narrow solid angle. Sweep rate—100 μsec/cm.

Figure 2 shows the oscilloscope traces of a generation pulse for various pumping levels. The splash visible at the beginning of generation is typical and is apparently due to a transient generation process.

The angular divergence of emission $\varphi_{div} \approx D/l \approx 6 - 8°$. According to (1) the number of excited modes is $L \approx (D^2/l\lambda)^2 \approx 2 \times 16^6$. The average intensity of output emission $I \approx 1\ kW/cm^2$ corresponding to the average number of photons in a mode $\langle n \rangle = IV/\hbar\omega cL(1 - r) \approx 10^6$.

2. Measurement of Intensity Fluctuation of Single-mode Emission

The primary aim of the experiment was to measure the single-mode emission intensity distribution function and to compare it with the theoretical distribution (23) that for $\langle n_l \rangle \gg 1$ has the form

$$p^{n_l} = \frac{1}{\langle n_l \rangle} \exp\left(-\frac{n_l}{\langle n_l \rangle}\right). \qquad (25)$$

To record emission intensity in a single mode we must observe the emission in a narrow (diffraction) angle $\varphi_{diff} \approx \lambda/D$. For this purpose the photomultiplier should be shielded by a disphragm with an opening $d \approx \lambda h/D$ where h is the distance from the output face of the laser to the diaphragm. This is equivalent to the requirement that the photomultiplier diaphragm not exceed the emission coherence area which is determined by the expression[12]

$$a_{coh} \approx \frac{\lambda}{D/h}, \qquad (26)$$

where D/h is the angle subtended by the emitting laser face at the diaphragm (we assume that $\varphi_{div} > D/h$). The required size of the diaphragm turns out to be very small (for example if $h = 100$ cm, $\alpha_{coh} \approx 0.04$ mm). This difficulty can be resolved by limiting the size of the emissive area at the laser face with an

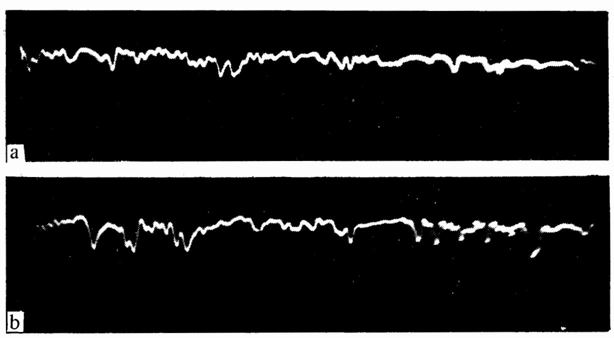

FIG. 4. Oscillographic traces of short intervals of the emission pulse within a narrow solid angle taken 100 (a) and 400 (b) μsec after start of generation. Sweep is 500 nsec across entire range.

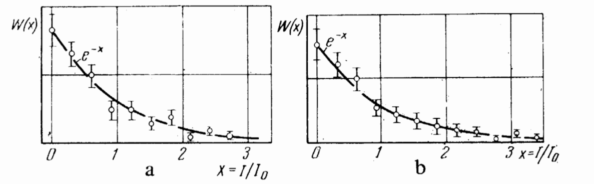

FIG. 5. Probability distributions of emission intensity fluctuations within a narrow solid angle (solid line denotes theoretical distribution) obtained by an appropriate processing of the oscilloscopic traces in Figs. 4a and b.

additional diaphragm whose diameter is $d_1 \ll D$. Then the maximum allowable diameter of the second diaphragm is $d_2^{max} \approx \lambda h/d_1$. In our experiment h = 60 cm, d_1 = 0.5 mm, and consequently $d_2^{max} \approx 0.8$ mm. To obtain a reliable recording of single-mode emission only we selected the diameter of $d_2 \approx 0.5$ mm.

Figure 3 shows an oscilloscope trace of an emission pulse separated out by the two diaphragms from a long sweep of 100 μsec/cm. The washed out picture of the curve indicates the presence of deep intensity fluctuations. The intensity fluctuation is seen in greater detail on traces obtained from a short sweep of 500 nsec/cm shown in Fig. 4. The oscilloscope traces correspond to two different time instants in the generation process (100 and 400 μsec).

Analysis of the oscilloscope traces yielded probability distributions of the intensity fluctuations W(I)[2)] Two typical distributions obtained from the traces in Fig. 4 are shown in Fig. 5. The experimental points show a satisfactory agreement with the theoretical distribution (25).

The analysis of these traces shows that the intensity fluctuation correlation time (coherence time) $\tau_{corr} \approx 10^{-8}$ sec. This corresponds to a generation line width

$$\Delta\nu \approx (2\pi\tau_{corr})^{-1} \approx 16\,\text{MHz} \tag{27}$$

Thus the obtained width of the generation line matches the width of the generation line of a nonresonant feedback laser in the nonstationary region that is determined by the expression found in [3]:

$$\Delta\nu = \Delta\nu_0 / \sqrt{\varkappa_0 vt / \ln 2}, \tag{28}$$

where $\Delta\nu_0$ is the width of the ruby luminescence line and v is the velocity of light in the resonator. In our case $\Delta\nu_0 \approx 0.5$ cm^{-1} = 1.5×10^{10} Hz, $\kappa_0 \approx 0.5$ cm^{-1}, v = 1.7×10^{10} cm/sec and consequently 10^{-4} sec after the start of generation $\Delta\nu \approx 5 \times 10^{-4}$ cm^{-1} = 15 MHz.

The fluctuation correlation time measured at various times after the start of generation (within the interval t = (1 – 4) $\times 10^{-4}$ sec) shows that correlation time increases with time and is in qualitative agreement with (28). We note that initially ($t < 10^{-5}$ sec) the emission line is so wide as to render the correlation time much shorter than the time constant of the photomultiplier. This should cause a smoothing of the photocurrent fluctuation at the leading edge of the pulse, a noticeable feature in Fig. 3.

3. Measurement of Emission Intensity Fluctuation in Several Modes

The relative amplitude of the fluctuations should decrease when the number of modes $\mathfrak{L}$ of the recorded emission is increased. When $1 \ll \mathfrak{L} \ll L$ (where L is the total number of modes in the laser) the relative amplitude of the fluctuations decreases according to $1/\sqrt{\mathfrak{L}}$. However as $\mathfrak{L}$ increases, when $\mathfrak{L} \approx L$, the saturation effect takes hold and the fluctuation amplitude decreases down to the limiting value determined by (17). In our experiment we measured the average fluctuation amplitude as a function of the number of modes $\mathfrak{L}$ of the recorded emission within the region $\mathfrak{L} \ll L$ ($\mathfrak{L}_{max} \approx 25$, $L \approx 2 \times 10^6$). The method of the experiment barred us from the region $\mathfrak{L} \approx L$.

The number of modes of the recorded emission was increased by expanding the diameter of the second diaphragm D_2. Figure 6 shows the average amplitude of the intensity fluctuation as a function of the second diaphragm diameter d_2 for the same average emission intensity I. The principal error of the measurement is determined by the accuracy of maintaining the constant level of the average intensity I. The diameter circumscribing maximum fluctuations, d_2 = 1 mm, is in agreement with the area of coherence of the emission passed through diaphragm D_1:

$$a_{coh} \approx \lambda h / d_1 = 0.8\,\text{mm}. \tag{29}$$

The experimentally observed decrease in the fluctuations amplitude δI is in qualitative agreement with the relationship $\delta I/I = 1/\sqrt{\mathfrak{L}} = \lambda h/d_1 d_2$. More accurate measurements of the dependence of the fluctuation amplitude on the number of modes including the region $L \approx L$ can apparently be performed only using a continuous-wave laser.

CONCLUSION

The present paper reports on the statistical properties of a nonresonant feedback laser. It is shown theoretically and experimentally that the intensity of emission in a narrow solid angle corresponding to a single-mode emission is subject to deep fluctuations whose distribution function coincides with the Bose-Einstein distribution for black-body radiation. It is shown theoretically that the emission intensity of the laser is fairly stable over the entire solid angle. The amplitude of the fluctuations is much lower than that of black-body radiation in the same angle.

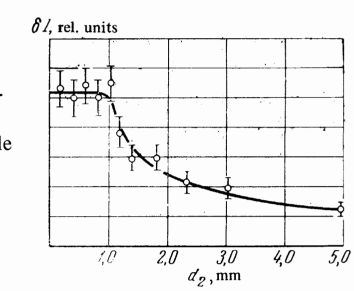

FIG. 6. Variation of the average amplitude of intensity fluctuations with increased solid angle (increased diameter d_2 of the second diaphragm) of the recorded emission (d_1 = 0.5 mm, h = 60 cm).

[2)] Strictly speaking the quantity that is measured in the experiment is the distribution function for fluctuations of the photocurrent, while the photon distribution function is related by the Mandel [13] formula to the photoelectron distribution function. However if photon distribution has the form (25), the stochastic nature of the "photon-photoelectron" relation does not affect the shape of the distribution function [14].

The presence of intensity fluctuations of the emission from a nonresonant feedback laser similar to emission fluctuations from noncoherent sources makes it possible to set up correlation experiments of the Brown-Twiss type [15] and to use correlation methods of measuring spatial and temporal coherence of emission [12].

In conclusion the authors express their deep gratitude to Academician N. G. Basov for his support and review of this work.

[1] R. V. Ambartsumyan, N. G. Basov, P. G. Kryukov, and V. S. Letokhov, ZhETF Pis. Red. **3**, 261 (1966) [JETP Lett. **3**, 167 (1966)]: Zh. Eksp. Teor. Fiz. **51**, 724 (1966) [Sov. Phys.-JETP **24**, 481 (1967)].

[2] R. V. Ambartsumyan, N. G. Basov, P. G. Kryukov, and V. S. Letokhov, IEEE J. of Quantum Electronics **QE-2**, 442 (1966).

[3] R. V. Ambartsumyan, P. G. Kryukov, and V. S. Letokhov, Zh. Eksp. Teor. Fiz. **51**, 1669 (1966) [Sov. Phys.-JETP **24**, 1129 (1967)].

[4] R. V. Ambartsumyan, P. G. Kryukov, V. S. Letokhov, and Yu. A. Matveets, ZhETF Pis. Red. **5**, 378 (1967) [JETP Lett. **5**, 312 (1967)].

[5] V. S. Letokhov, Zh. Eksp. Teor. Fiz. **53**, 2210 (1967) [this issue, p. 1246].

[6] J. A. Fleck, Jr., Phys. Rev. **149**, 309 (1966).

[7] J. A. Fleck, Jr.,,Phys. Rev. **149**, 322 (1966).

[8] V. S. Letokhov, ZhETF Pis. Red. **5**, 262 (1967) [JETP Lett. **5**, 212 (1967)]; Zh. Eksp. Teor. Fiz. **53**, 1442 (1967). [Sov. Phys.-JETP **26**, 835 (1968)].

[9] J. A. Armstrong and A. W. Smith, IBM J. Res. and Develop. **10**, 225 (1966); Phys. Lett. **19**, 651 (1966).

[10] T. J. Bridges and W. W. Rigrod, IEEE J. of Quantum Electronics **QE-1**, 303 (1965).

[11] A. L. Schawlow, Advances in Quantum Electronics, ed. by J. R. Singer, N. Y. 1961.

[12] E. Wolf and L. Mandel, Revs. Modern Phys. **37**, 231 (1965); Usp. Fiz. Nauk **87**, 491 (1965).

[13] L. Mandel, Proc. Phys. Soc. **72**, 1037 (1958).

[14] V. S. Letokhov, Zh. Eksp. Teor. Fiz. **50**, 765 (1966) [Sov. Phys. JETP **23**, 506 (1966)]; Preprint FIAN, A-45 (1965).

[15] R. Hanbury Brown and R. Q. Twiss, Nature **177**, 27 (1956).

Translated by S. Kassel
223